

TIME DEPENDENT MHD MODELS FOR ALUMINIUM REDUCTION CELLS

V. Bojarevics and K. Pericleous

University of Greenwich, Park Row, London SE10 9LS, UK

Keywords: electrometallurgy, aluminium reduction cells, waves, magnetohydrodynamics

Abstract

Time dependent MHD or stability problems for the aluminium reduction cells are typically restricted to the mathematical developments without the inclusion of the electrolyte channels. However, according to the well known Moreau-Evans model, the presence of electrolyte channels increases very significantly the stationary interface deformation. In this paper general time dependent theory and numerical modelling of an aluminium cell is extended to the case of variable bottom of aluminium pad and variable thickness of electrolyte to account for the channels. Instructive analysis is presented for multi-physical coupling of the magnetic field, electric current, velocity and wave development by animated examples for the high amperage cells. The results indicate that the 'rotating wave' instability is dominant in simplified cases not accounting for the effect of channels. The effect of channels creates a stabilizing effect, resulting in a 'sloshing', parametrically excited MHD wave development in aluminium reduction cells.

Introduction

Magneto Hydro Dynamic (MHD) problems for aluminium electrolysis cells are of increasing importance with the rise of the amperage in the modern cells. The electric current, interacting with the associated magnetic field, creates agitating effects limiting the cell productivity, and can cause an instability of the interface between liquid aluminium and electrolyte. This can cause significant electrical energy loss, disruption in the technology and increase of environmental pollution rate. The time dependent MHD or stability problems for the aluminium reduction cells are usually treated as simplified mathematical models restricted to a bare minimum of the essential interacting physical factors, like simplified magnetic field, electric current distribution, cell geometry, neglecting turbulent velocity field, etc. One of the significant neglected physical factors for the stability problems of aluminium electrolysis cells is the absence of the electrolyte channels, see for example [1-4]. In the stationary case without waves Moreau and Evans [5] introduced a model for the electrolyte channels surrounding the anodes, their influence on the horizontal flow circulation and the metal-bath interface deformation. According to their model the interface deformation in the stationary case increases very significantly when the electrolyte channels are accounted for.

The variable bottom effects and the horizontal circulation interaction with the waves are widely investigated in the sea wave studies using shallow water models [6]. Recently a theory and a numerical model of the 'shallow layer' electrolysis cell was extended to the cases of variable bottom of aluminium pad and the variable thickness of the electrolyte due to the anode nonuniform burn-out process and the presence of the side channels [7]. However, in this paper the free surface on top of the electrolyte channels was not accounted for, effectively assuming that the rigid lid surface condition is imposed both for the channels and the solid anode bottom.

The problem of the interface calculation became apparent in the light of the recent paper [8] providing a 'benchmark' test for the stationary interface and the velocity field in liquid metal. During the first attempts to apply the numerical model [7] to the 'benchmark' case we obtained a

good correspondence to velocity field and the electric current results, but the interface shape initially was quite different from that presented in [8]. Therefore we reconsidered the theory by including the free surface effects for the bath filled deep channels, effectively extending the Moreau-Evans model to the non-stationary case. The new version is directly applicable to the previous full nonlinear wave model and the dynamic interaction with the electromagnetic field as it is implemented in the MHD numerical code suitable for commercial high amperage cell modelling.

New model for the time dependent interface

In the present extension of the ‘shallow water’ theory for variable depth of two fluid layers with a common interface we will assume that the layer deformation is small, except for the channels whose effect will be expressed as a hydrostatic ‘connected vessels’ principle. The shallow water model derivation starts with the assumption that for a small depth of fluid the vertical momentum equation reduces to quasi-hydrostatic equilibrium between the vertical pressure gradient ∇p and the gravity force ρg . After integrating along the vertical coordinate z :

$$p(x, y, z) - p(H) = -\rho g(z - H), \quad (1)$$

where the reference height $H(x, y, t)$ can be chosen to coincide with the common surface for both liquid layers – the unknown interface between the metal and the electrolyte layers. The gradient in the horizontal direction of the hydrostatic pressure distribution does not depend on vertical coordinate in the respective layer, as can be seen from (1). If the top surface of the bath layer is denoted as H_t , then the pressure at the top of channels covered by a rigid lid could be obtained by solving the horizontal momentum equations. However, if there is a free surface on top of the electrolyte channels, then $p(H_t) = 0$, and the pressure at the variable interface $H(x, y, t)$ is related by the hydrostatic condition (1) at the local horizontal position:

$$p(H) = \rho_2 g(H_t - H(x, y, t)), \quad (2)$$

where for clarity we added the index ‘2’ for the electrolyte properties. According to the Moreau & Evans [5], the top surface H_t in the channels is practically flat and equal in all the electrolyte channels. If the channels (side, middle and between the individual anodes) are sufficiently deep, say 2-3 or more times the average anode-cathode distance (ACD), then this hydrostatic pressure will be effectively dominating contribution in the whole electrolyte layer, similarly to ‘connected vessels’ principle. The electromagnetic force in the electrolyte will add only a smaller order of magnitude modification to this dominant hydrostatic pressure. From the equation (2) then follows an approximated leading order horizontal pressure gradient variation in the electrolyte at the variable interface $H(x, y, t)$:

$$\partial_x p(H) = -\rho_2 g \partial_x H; \quad \partial_y p(H) = -\rho_2 g \partial_y H. \quad (3)$$

With these approximations for the pressure and its horizontal gradient in both shallow layers, we can express the horizontal momentum equations for the depth average non-dimensional quantities. Initially we will consider the stationary case only. The Moreau & Evans model [5] is based on the linear equations for the two fluid layers:

$$0 = -\partial_j p - \mu \hat{u}_j + \hat{f}_j; \quad \partial_j \hat{u}_j = 0, \quad (4)$$

where the indexes $j = (1 \text{ or } 2)$ represent respectively x and y coordinates, the summation over repeated indexes j means the divergence free depth average velocity field. After substituting the depth independent pressure gradient from (3), the horizontal momentum equations are

$$0 = -\partial_j p(H) - \rho_j g \partial_j H - \mu \hat{u}_j + \hat{f}_j . \quad (5)$$

The common pressure $p(H)$ at the interface can be eliminated by taking the difference between the equations in the two layers, characterized each by the respective index: $i=1$ (aluminium) and $i=2$ (electrolyte). The unknown interface shape will be determined by solving the resulting equations coupled to the velocity field. When the channels are absent, the friction coefficient μ can be assumed as a constant in each layer, and the equation (5) gives the second order equation for the interface:

$$(\rho_1 - \rho_2) g \partial_j H = \partial_j (\hat{f}_{j1} - \hat{f}_{j2}) . \quad (6)$$

The boundary conditions are derived from (5) using zero normal velocity condition at the cell walls. However, in the presence of the bath channels the approximation of a constant friction coefficient is not valid, dropping sharply to a very low value in the channels. Therefore the divergence operator applied to (5) will not eliminate the velocity field from the interface equation. The coupling to the intense velocity near the channels can be eliminated, to the hydrostatic approximation accuracy discussed previously (3). Applying the hydrostatic pressure gradient (3) directly in the equation (5) for the aluminium ($i = 1$) layer only:

$$0 = -(\rho_1 - \rho_2) g \partial_j H - \mu_i \hat{u}_{1j} + \hat{f}_{1j} . \quad (7)$$

The continuity of the pressure at the interface is already satisfied by choosing the pressure $p(H)$ at the common interface. The bottom friction coefficient in the aluminium is constant according to the Moreau & Evans model, and the divergence of (7) gives the stationary interface equation in the case with deep electrolyte channels having free top surface:

$$(\rho_1 - \rho_2) g \partial_{jj} H = \partial_j (\hat{f}_{j1}) . \quad (8)$$

The horizontal circulation velocities, driven by the rotational part of the electromagnetic force, can be calculated by solving the momentum equations in the two layers. Additionally in a more general approach, the 2-equation (e.g. $k-\varepsilon$) turbulence model can be applied for the horizontal turbulent momentum diffusion (the effective viscosity). We will not consider here this part of the theory (see [7]), instead focusing on the time dependent interface evolution equation.

Taking into account the hydrostatic pressure distribution in the presence of the channels for the full time dependent interface equation stated previously in [7], we have the non-linear wave equation for the aluminium-electrolyte interface $H(x,y,t)$ with the variable bottom $H_b(x,y)$ and top $H_t(x,y)$:

$$\begin{aligned} & \left(\frac{\rho_1}{H - H_b} + \frac{\rho_2}{H_t - H} \right) \partial_{tt} H + \left(\frac{\rho_1 \mu_1}{H - H_b} + \frac{\rho_2 \mu_2}{H_t - H} \right) \partial H - (\rho_1 - \rho_2) g \partial_{jj} H \\ & = \partial_j (-\hat{f}_{j1}) - \frac{1}{2} (H - H_b) \partial_{jj} \hat{f}_{z1} - [\rho_1 \partial_j (\hat{u}_{k1} \partial_k \hat{u}_{j1}) - \rho_2 \partial_j (\hat{u}_{k2} \partial_k \hat{u}_{j2})] \end{aligned} \quad (9)$$

The linear stability models can be recovered from (9) by excluding the nonlinear horizontal velocity

term (containing the rotational and potential parts), the vertical electromagnetic force component f_z contribution, and assuming the H_b and H_t as constants. The nonlinear equation (9) extends the wave description to the cases of variable top and bottom, in the presence of electrolyte channels. The complexity of any practically usable MHD model arises from the coupling of the various physical effects: fluid dynamics, electric current distribution, magnetic field and thermal field. Magnetic field in an aluminium cell is created by the currents in the cell itself and from the complex bus-bar arrangement around the cell, in the neighboring cells and the return line, and by the effect of cell construction steel magnetization. The general MHD model, presented previously in [7] and references therein, accounts for the time dependent coupling of the current and magnetic fields with the bath-metal interface movement. The magnetic field from the currents in the full bus-bar network is recalculated at each time step during the dynamic simulation using the Biot-Savart law.

Numerical results for 180 kA and 500 kA cells

The numerical solution of the described MHD model uses a mesh of 128x64x2 and a spectral function representation for each fluid layer. This ensures sufficient accuracy of solution, while permitting to re-compute the time dependent distribution of electromagnetic and velocity fields in a reasonable computational time. The numerical model was successfully tested [9] against the 'benchmark' test [8] regarding the stationary fields. The test involved an assumed distribution of stationary electric current supply to the top and bottom of the liquid and a given magnetic field. For a more realistic case, similar to many commercial cells, we will present a comparison of two cases with the full bus-bar arrangement around the cell, accounting for the time variation of the electric currents and magnetic field. The bus arrangement is presented in the Figures 1 and 2 showing side by side comparison of the two cells: a relatively small 180 kA and much larger 500 kA cells. The cells are arranged side by side in the full pot-line with a return line. Only the active simulation cell is shown, but the magnetic field from the adjacent cells is included in the full simulation. The other noticeable feature of the model is the presence of the steel shell made of magnetizable material, which is fully accounted for by a finite element discretization and iterations over the user prescribed non-linear magnetization curve. The computed magnetic field is 3-dimensional and changes in time if the electric currents fluctuate with the waves at the electrolyte-metal interface. The computed magnetic field at the top and bottom of liquid metal for the smaller 180 kA cell is shown in Figures 3 and 4, which demonstrates the importance of the depth dependence of the magnetic field in the fluid layer.

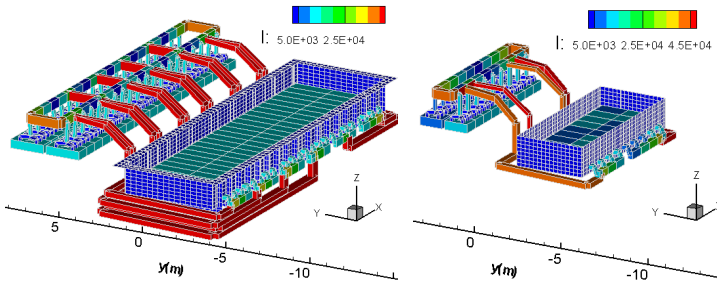


Figure 1. Left: busbar arrangement for the 500 kA cell generated by the numerical model.
Figure 2. Right: busbar arrangement for the 180 kA cell shown to the same scale as in Figure 1.

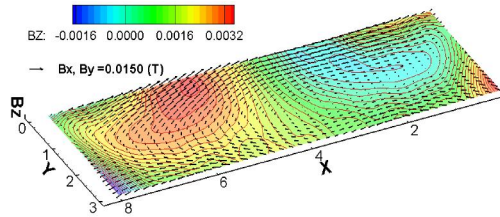


Figure 3. Magnetic field at the top of liquid metal for 180 kA cell.

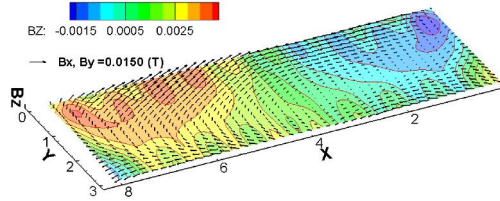


Figure 4. Magnetic field at the bottom of liquid metal for 180 kA cell.

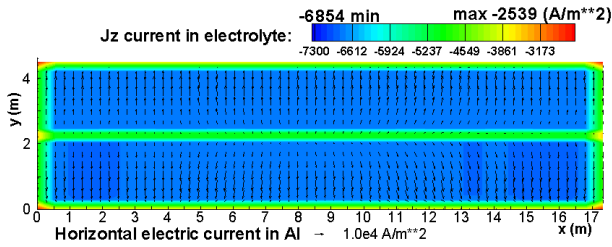


Figure 5. The electric current in liquid electrolyte with the channels at initial stage for 500 kA cell.

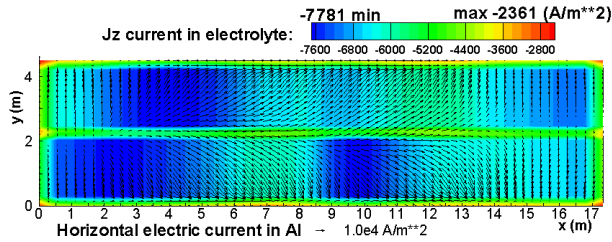


Figure 6. The computed electric current in liquid electrolyte with the channels at later stage of wave development with the anode burn-out activated for 500 kA cell.

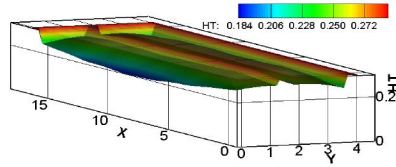


Figure 7. The computed anode bottom in contact to the liquid electrolyte with the channels for 500 kA cell after the burn-out option is activated.

The electrolyte channels affected significantly the electric current distribution in the electrolyte layer is, as can be seen from the Figure 5. In addition to that, when the metal-electrolyte interface is deformed or in a wave development process, this is instantaneously reflected in the electric current distribution as shown in the Figure 6. The usual argument, that the electric current distribution will be smoothed out with the anode bottom acquiring the shape of the time average interface shape, is true only partially because of the time dependent nature of the wave process. The numerical model includes the option to account for the anode bottom burn-out according to the time-average or stationary interface shape (Figure 7).

The electromagnetic force distribution as computed for the electric current and the resulting magnetic field shows that the overall force distribution and magnitude are quite similar in both fluid layers. There is practically a balance between the ‘pinching’ effects of the forces in the two layers. Therefore it is not surprising to find for the case without the effect of the electrolyte channels that the interface deformation is very small and slightly inflected in the middle (because of a slightly larger force concentration in electrolyte), as shown in the Figure 8. A strikingly different interface deformation (Figure 9) is obtained when using the model equation (8), or even (9), with the hydrostatic pressure dominating in the electrolyte. The result is validated by the published ‘benchmark’ results [8,9].

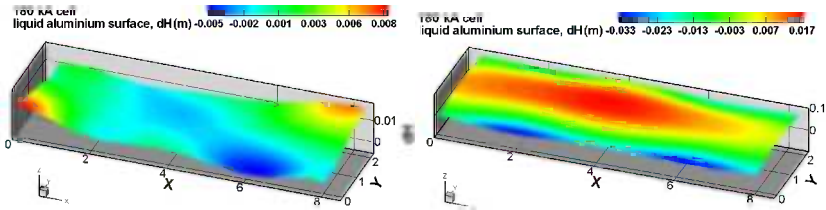


Figure 8. (Left) The computed metal-bath shape for 180 kA cell without the open channel effect.

Figure 9. (Right) The computed metal-bath shape for 180 kA cell with the open channel effect.

For further tests the velocity fields were computed. The computed velocity in the electrolyte [9] is very similar qualitatively to that predicted by Moreau & Evans [2], clearly showing the effects of the intense recirculation in the channels. The flow is sufficiently intense and develops significant turbulence, which leads to a redistribution of the velocity field. The established velocity field for the aluminium layer [9] is very similar to that predicted in [8] as a part of the ‘benchmark’ tests.

The full MHD time dependent code includes continuous coupling of the electrodynamic and hydrodynamic fields. The horizontal electric currents in the liquid metal affect the magnetic field, making it 3-dimensional and different at the top and bottom of the metal layer (Figures 3 and 4).

Initially the deformation of the liquid metal surface is computed from the electric current given for a flat interface, with or without the effect of electrolyte channels, leading to what is usually assumed to be a 'stationary' interface. The time development of the coupled fields shows that the waves are initiated and may continue to grow in amplitude or are gradually damped depending on the distribution of the magnetic field in a particular cell. The cases without the inclusion of the electrolyte channels demonstrate that the instability sets in more easily, and in the extreme case the time when the wave crest reaches the anode bottom is shorter (Figure 10). The instability type in the case without the channels is the classical rotating wave (see Figures 8 and 11), as described in the theoretical papers [1-4]. The presence of the electrolyte channels changes the instability type, which resembles more a 'sloshing' wave constrained along the middle longitudinal line of the cell (Figures 9 and 12). The magnetic field for the 500 kA cell is better optimized for the stability purpose, therefore the waving is of a smaller amplitude and not growing with time (Figure 13). The effect of the electrolyte channels is similar as in the smaller 180 kA cell: the channels increase the stationary deformation, but make the cell significantly more stable to the waves. An important observation is also deduced when running the full case with the time varying magnetic field. This case demonstrates the additional stabilizing effect of the magnetic field self-adjustment to the wave induced electric current redistribution. If the full 3-dimensional magnetic field is kept fixed as computed initially for the 'stationary' interface, as in many previous studies, the cell is far less stable.

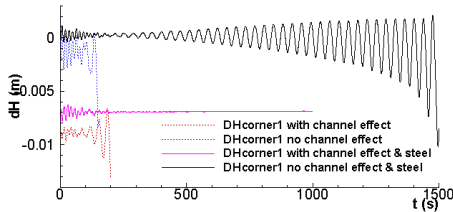


Figure 10. Different type of instability when the channels and steel are accounted in 180 kA cell.

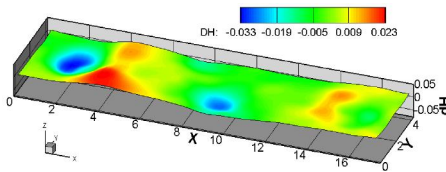


Figure 11. The computed metal-bath shape for 500 kA cell without the open channel effect.

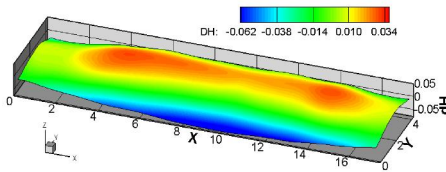


Figure 12. The computed metal-bath shape for 500 kA cell with the open channel effect.

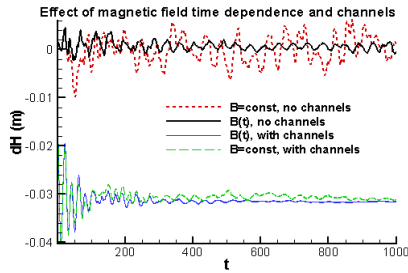


Figure 13. Waves in the 500 kA cell when the channels and magnetic field time dependence are accounted for.

Conclusions

The Moreau-Evans model can be extended to the case of non-stationary cell behavior. The inclusion of the electrolyte channels is crucial to predict the correct interface deformation both in the stationary case and the wave development. The full coupled electromagnetic and hydrodynamic simulation reveals new stabilizing effects.

References

1. Urata, N., Mori, K. and Ikeuchi, H. Behavior of bath and molten metal in aluminium electrolytic cell. *Keikinzo*, 26 (1976), no. 11, 573-600.
2. A. D. Sneyd and A. Wang. Interfacial instability due to MHD mode coupling in aluminium reduction cells. *J. Fluid Mech.*, 263 (1994), 343-359.
3. V. Bojarevics and M. V. Romerio. Long waves instability of liquid metal-electrolyte interface in aluminium electrolysis cells: a generalization of Sele's criterion. *Eur. J. Mech., B/Fluids*, 13 (1994), no 1, 33-56.
4. H. Sun, O. Zikanov, B. A. Finlayson and D. P. Ziegler. The influence of the basic flow and interface deformation on stability of Hall-Herault cells. *Light Metals 2005*, (TMS, 2005), 437-441.
5. R. Moreau and J.W. Ewans. An analysis of the hydrodynamics of aluminium reduction cells. *Journal of Electrochemical Society*, 131 (1984), no. 10, 2251-2259.
6. C. C. Mei. *The Applied Dynamics of Ocean Surface Waves* (World Scientific, 1989).
7. V. Bojarevics and K. Pericleous, "Shallow Water Model for Aluminium Electrolysis Cells with Variable Top and Bottom". In *Proceedings of TMS Light Metals* (2008), 403-408.
8. D.S. Severo, V. Gusberti, A.F. Schneider, E.C. Pinto and V. Potocnik, "Comparison of Various Methods for Modeling the Metal-Bath Interface". In *Proceedings of TMS Light Metals* (2008), 413-418.
9. V. Bojarevics and K. Pericleous, "Solutions for the Metal-Bath Interface in Aluminium Electrolysis Cells". In *Proceedings of TMS Light Metals* (2009), 569-574.